



## Molecular Docking Assessment of Clinically Approved Antiviral Drugs against M<sup>pro</sup>, Spike Glycoprotein and Angiotensin Converting Enzyme-2 Revealed Probable Anti-SARS-CoV-2 Potential

Temitope I. Adelusi<sup>1\*</sup>, Misbaudeen Abdul-Hammed<sup>2</sup>, Emmanuel M. Ojo<sup>1</sup>, Qudus K. Oyedele<sup>1</sup>, Ibrahim D. Boyenle<sup>1</sup>, Ibrahim O. Adedotun<sup>2</sup>, Olamide T. Olaoba<sup>3</sup>, Ajayi A. Folorunsho<sup>4</sup>, Oladipo E. Kolawole<sup>5</sup>

<sup>1</sup>Computational Biology/Drug Discovery Laboratory, Department of Biochemistry, Ladoké Akintola University of Technology, PMB 4000, Nigeria

<sup>2</sup>Computational Biophysical Chemistry Laboratory, Department of Pure and Applied Chemistry, Ladoké Akintola University of Technology, PMB 4000, Nigeria

<sup>3</sup>Laboratory of Functional and Structural Biochemistry, Federal University Sao Carlos, Sao Carlos, SP, Brazil

<sup>4</sup>Department of Physiology, College of Medicine, Ladoké Akintola University of Technology, PMB 4000, Nigeria

<sup>5</sup>Department of Microbiology, Laboratory of Molecular Biology, Immunology and Bioinformatics, Adeleke University, Ede, Osun State, Nigeria

### ARTICLE INFO

### ABSTRACT

#### Article history:

Received 12 February 2021

Revised 16 March 2021

Accepted 18 April 2021

Published online 03 May 2021

**Copyright:** © 2021 Adelusi *et al.* This is an open-access article distributed under the terms of the [Creative Commons Attribution License](https://creativecommons.org/licenses/by/4.0/), which permits unrestricted use, distribution, and reproduction in any medium, provided the original author and source are credited.

Ever since the novel SARS-CoV-2 coronavirus was identified at Wuhan in China, numerous researchers have been working on remedies to ameliorate the COVID-19 disease perpetrated by this deadly virus. Umpteen researchers engaged *in silico* approaches as a fast means of discovering drugs with potential inhibitory activity against SARS-CoV-2 to combat the COVID-19 pandemic. In this computational study, FDA approved antiretroviral, anti-Ebola, and anti-SARS drugs were docked against SARS-CoV-2 M<sup>pro</sup> (6LU7), Prefusion 2019-nCoV Spike glycoprotein (6VSB), the peptidase domain of human ACE2 (2AJF) and SARS-CoV 3CL protease (2ZU4) in order to detect the drugs with the best binding affinity for the active sites of these proteins. The top 3 drugs for each class of drugs show strong binding affinities from -7.5 - -9.2 Kcal/mol. The docking result shows the consistent score of Saquinavir, Amodiaquine, Clomiphene, Indinavir, Lopinavir, Maraviroc, Nelfinavir, and Verapamil across those proteins. However, our results indicate that indinavir, saquinavir and maraviroc with considerable binding affinity might be further optimized in preclinical and clinical studies to determine their role in the management of COVID-19. Furthermore, we noticed that the amino acid residues common to 6LU7-ligand complexes and 2ZU4-ligand complexes include Glu166, Cys145, and Met49. We therefore conclude that these residues could be critical to their functional and catalytic potentials. These residues could also be a critical component of their conserved domain that forms catalytic dyad because our result falls in line with others where His41 and Cys145 were reported to be conserved residues at M<sup>pro</sup> active site.

**Keywords:** - SARS-CoV-2, COVID-19, Anti-viral drugs, Molecular docking, Binding energies.

### Introduction

The severe acute respiratory syndrome coronavirus-2-mediated Coronavirus disease (COVID-19) is a pathogenic viral infection with a high transmittable character causing one of the most serious pandemics. Due to the similarities between SARS-CoV-2 and SARS-like bat viruses revealed from the phylogenetic analysis, it was proposed that bats could be the probable primary reservoir.<sup>1</sup> It originated from a city in Hubei province of Wuhan in China and the severity associated with the human-to-human transmission of 2019-CoV is currently posing serious death to the world.<sup>2,3</sup> This SARS-like pneumonia has been suspected to emerge from an unknown animal and to have subsequently been transmitted to humans in the seafood and wild animal market.

\*Corresponding author. E mail: [tiadelusi@lautech.edu.ng](mailto:tiadelusi@lautech.edu.ng)  
Tel: +2347067774039

**Citation:** Adelusi TI, Abdul-Hammed M, Ojo EM, Oyedele QK, Boyenle ID, Adedotun IO, Olaoba OT, Folorunsho AA, Kolawole OE. Molecular Docking Assessment of Clinically Approved Antiviral Drugs against M<sup>pro</sup>, Spike Glycoprotein and Angiotensin Converting Enzyme-2 Revealed Probable Anti-SARS-CoV-2 Potential. Trop J Nat Prod Res. 2021; 5(4):778-791. [doi.org/10.26538/tjnpr/v5i4.30](https://doi.org/10.26538/tjnpr/v5i4.30)

Official Journal of Natural Product Research Group, Faculty of Pharmacy, University of Benin, Benin City, Nigeria.

The RT-PCR amplicons-mediated phylogenetic analysis of five infected patients and full genome next generation-orchestrated sequencing unravel the novelty of this virus which was elucidated to be close to the SARS-associated coronaviruses in the Chinese horseshoe bats.<sup>2</sup> History validates that SARS in 2002, 2012 Middle East respiratory syndrome and the 2017 swine acute diarrhea that caused serious infectious diseases in both humans and livestock are all descendants of bats coronaviruses (CoVs). Further epidemiological-related studies were carried out using virome analysis for the classification of CoVs from 15 Yunnan and 831 bats species at Guanxi, Sichuan Province. It was reported that out of 22 individual samples of four (4) bat species, 11 CoVs strains were identified which include 4  $\alpha$ -CoVs from Guangxi's *Scotophilus kuklii* strictly associated with already reported bat CoV and PEDV (Porcine Epidemic Diarrhea Virus). These findings signify the existence of a lineage that could be traced back to bats under the genus Alphacoronaviruses.<sup>4</sup> Besides the spread of this virus throughout the whole Country of China from Wuhan City,<sup>5</sup> it has rapidly spread to other countries. For SARS-CoV and some SARS-like bats coronaviruses, angiotensin-converting enzyme II (ACEII) serves as their cell receptor.<sup>11</sup> It was further reported from genomic studies that the SARS-CoV-2's receptor-binding domain was significantly similar to that of SARS-CoV. This critically points at the fact that human ACE2 receptor could be exploited as the gateway for coronaviruses into human cells.<sup>12,13</sup> The very first recovery from this disease emanated from a remdesivir-administered (an anti-Ebola drug) patient in the United States after

which the Chinese also put this drug into clinical trial with the aim of approving its implementation in clinical therapeutics for COVID-19. Therefore, this signifies a probable groundbreaking anti-coronaviral potential of clinically approved anti-Ebola drugs. Besides this, it was recently reported that an Ebola-related filovirus was found in Chinese bats (*Pteropodidae*).<sup>14</sup> This also logically explains a probable relationship between Ebola virus and COVID-19. This same drug inhibited the replication of SARS-CoV-2 when taken alone or in combined therapy with chloroquine or interferon- $\beta$  and patients were declared clinically recovered.<sup>15-18</sup> Furthermore, homologous recombination analysis revealed that the coronavirus glycoprotein spike that binds to the host receptor originated from an unknown  $\beta$ -coronavirus SARS-CoV (CoVZXC21/CoVZC45)<sup>19</sup>. Therefore, we believe obstruction of SARS-CoV-2 components used for host binding and replication could help inhibit the infection and nip it in the bud. However, it takes decades and several millions of dollars to design efficient novel drugs to reduce the pathogenic activities of this virus via a conventional drug discovery approach. Due to the current emergency situation, a promising alternative that relies upon computational approach to facilitate reliable results in less time is needed. Therefore, recent advances in drug discovery repurposes existing drugs via *in-silico* techniques such as virtual screening. Target selection and validation are crucial steps in drug repurposing approach. We selected 3cl<sup>pro</sup> which is the viral main protease, Spike glycoprotein which has the receptor binding domain that can attach to the host receptor, ACE2 which is the host cellular receptor, and SARS-COV that serves as a positive control.

From a plethora of literature, we selected 23 compounds with anti-retroviral, anti-Ebola and anti-SARS activities which are significant for the present study. In this *in silico*-based research, our aim is to screen some FDA approved drugs against 6LU7 (SARS-CoV-2 Main protease), 2ZU4 (SARS-CoV-1 Main protease), 6VSB (Spike glycoprotein), and 2AJF (Angiotensin Converting Enzyme 2) using molecular docking approach in order to figure out the best drugs with probable propensities to emerge as anti-COVID-19 therapy. Our aim is to emphasize the molecular reasons why some of these antiviral drugs could be repurposed for the management/treatment of SARS-CoV-2-mediated COVID-19.

## Materials and Methods

### Ligands preparation

For docking against the SARS-COV and SARS-COV-2 main protease, Spike glycoprotein, and ACE2 proteins, the Drug bank chemical library was used. This is public repository accessible online containing information of compounds and their biological activities. The 3D structures were downloaded in SMILE format from the database and converted individually to PDB files using CACTUS online translator ([www.cactus.nci.nih.gov](http://www.cactus.nci.nih.gov)). These compounds were preprocessed using python script prepared for docking studies with the aid of Autodock vina (MGL tool 1.5.6)<sup>22</sup> which is an efficient computational tool to generate PDBQT format.

### Protein preparation

The crystallographic structure 6LU7, 2ZU4, 6VSB, and 2AJF of a minimal resolution used for this study were retrieved from Protein Data Bank ([www.rcsb.org](http://www.rcsb.org)), after which the water molecules of these proteins were removed using Discovery Studio version 19.1. Autodock vina (MGL tool 1.5.6)<sup>22</sup> was used to prepare these proteins, then the addition of Hydrogen bonds and Geisteiger charges were added to generate the PDBQT files.

### Active site prediction and validation

Two online tools were used to predict the active site of each protein. CASTp<sup>23</sup> was used to predict the amino acids that occupy the binding pocket of each protein after which COACH was used to validate these residues for consistency.

### Molecular docking protocol

Molecular docking helps predict the predominant binding pose of a ligand with a protein and analyze the binding interactions between

them. Keeping the docking parameters as default, rigid docking was done by defining the grid box with dimension around active sites of each protein and the exhaustiveness was also kept at 8. For SARS-COV and SARS-COV-2, the grid box was set at 60x60x60, then 80x80x80 was set for both Spike glycoprotein and ACE2. The ligands were evaluated based on their respective binding affinity and molecular interactions were analyzed using Pymol and Discovery Studio<sup>24</sup>. For accuracy, all our docking experiments were done with AutoDock Vina on a Windows 8 workstation, 4GB RAM, 2.1GHZ with 500GB HDD Intel Core i3.

## Results and Discussion

Twenty-three (23) clinically approved drugs which include eight (8) antiretroviral (baricitinib, darunavir, efavirenz, fosamprenavir, lopinavir, maraviroc, remdesivir, and saquinavir), seven (7) anti-Ebola (amiodarone, amodiaquine, chloroquine, clomiphene, dronedarone, toremifene, and verapamil) and eight (8) anti-SARS (acyclovir, graciclovir, ribavirin, indinavir, nelfinavir, osaltamivir, saquinavir, and zanamivir) were docked against COVID-19 protein (PDB code: 6LU7) and (PDB code: 2ZU4) and the result of the top 2 compounds of each categories of drugs is presented as figure 2 and 3 showing the various interactions and the binding pockets. In order to screen for the probable strongest clinically approved antiviral drugs that could be potential anti-COVID-19 candidates, we investigated the binding energies predicting the affinity of the ligands for the proteins and the interactions (conventional hydrogen bond, carbon-hydrogen bond, pi-pi stacked, pi-alkyl and pi-sulphur interactions) (Figure 2) This was done together with the pocket's active sites of each of the proteins expressing the conformation of the ligand with highest binding energy and its binding with the active pocket of the protein as presented in Figure 2. When antiretroviral drugs were docked against 6LU7, maraviroc (-7.7 Kcal/mol) and lopinavir (-7.1 Kcal/mol) showed the least binding energies while for anti-ebola, amodiaquine (-6.0 Kcal/mol) and verapamil (-5.5 Kcal/mol) exhibited the least binding energies. Out of all the Anti-SARS drugs, saquinavir (-7.5Kcal/mol) and nelfinavir (-6.3 Kcal/mol) had the least binding energies when docked against 6LU7. It must be noted that Maraviroc had the least binding energy when compared to all the ligands and the N3 standard (-7.6 Kcal/mol). These same sets of clinically approved drugs were docked against 2ZU4 and the result is presented as Figure 3. It was found that lopinavir (-7.8 Kcal/mol) and Maraviroc (-7.2 Kcal/mol) had the least binding energies among the antiretroviral drugs while verapamil (-7.4 Kcal/mol) and clorophene (-6.5 Kcal/mol) showed the least for anti-ebola drugs.

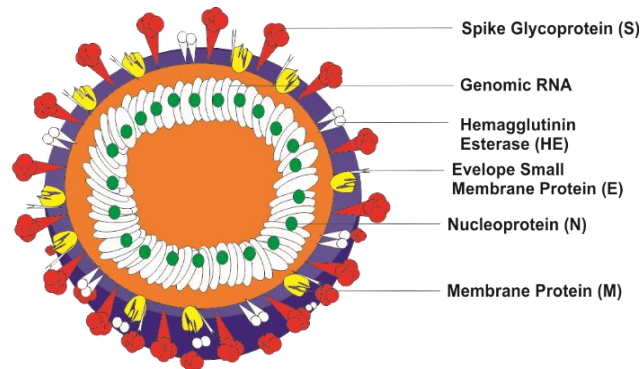


**Figure 1:** Structure of SARS-CoV-2 (Severe Acute Respiratory Syndrome Coronavirus-2).

This spherical enveloped particle with single-stranded positive-sense RNA that associates itself with a nucleoprotein consist of the spike club-shaped glycoprotein S, membrane protein M, envelope E and nucleocapsid N proteins which are structural proteins responsible for SARS-CoV-2 assemblage, infection and genome maintenance. The spike glycoprotein facilitates its attachment to the host cells which

when acted upon by host proteases cleave into N-terminal (S1) and C-terminal (S2) subunits.<sup>20,21</sup>

For anti-SARS, nelfinavir (-7.8 Kcal/mol) and saquinavir (-7.3 Kcal/mol) were the least against 2ZU4 among the eight (8) anti-SARS drugs. We also noted that all the ligands had better binding energies when compared to the standard.

The same 23 drugs were docked against 6VSB (2019-nCoV spike glycoprotein) and 2AJF (Angiotensin-Converting Enzyme 2) host cellular receptor and the results for the best two (2) compounds under each categories of FDA clinically approved drugs are presented as Figure 4 and Figure 5 showing the various interactions between the ligands and respective protein with their active binding. For anti-retroviral drugs, lopinavir (-7.7 Kcal/mol) and maraviroc (-7.4 Kcal/mol) had the least binding energies when docked against 6VSB while for anti-ebola drugs, amodiaquine (-5.9 Kcal/mol) and verapamil (-5.4 Kcal/mol) were the best and lastly nelfinavir (-7.1 Kcal/mol) and indinavir (-6.8 Kcal/mol) were the best for anti-SARS drugs. In addition, when all these were compared to the standard 2-(acetylamino)-2-deoxy-A-D-glucopyranose [-5.5 Kcal/mol for 6VSB], we noticed that all ligands had lower binding energies than the standard.

There was significant increase in binding affinities of all the best 2 ligands against ACE2. Maraviroc and lopinavir had close affinity of -8.5 Kcal/mol and -8.3 Kcal/mol. Verapamil and chlorophene had binding affinity of -6.8 Kcal/mol and -6.4 Kcal/mol, respectively. Indinavir (-9.2 Kcal/mol) and Saquinavir (-9.1 Kcal/mol) possessed highest affinity when compared with 2-(acetylamino)-2-deoxy-alpha-D-glucopyranose, a substrate standard of ACE2 (-4.5 Kcal/mol).

Table 2 illustrates the amino acid interactions existing between the selected low binding energy ligands and the proteins (the complexes). Maraviroc interacted with 6LU7 at Glu166, His41, Cys145, Met49, Pro168, Gln189, Tyr54, Arg188, and Asp187 forming only one hydrogen bond with Tyr54; nelfinavir at Gln189, His41, Cys145, Leu27, Met49, and Met165 forming one hydrogen bond with Gln189; saquinavir at Tyr126, Asp289, Phe291, Lys5, and Ala285 with one hydrogen bond (Glu288); lopinavir at Glu166, His41, Cys145, His164, Gln189, Met49, and Thr190 forming three (3) hydrogen bonds with Cys145, Gln189, and His164; amodiaquine at Lys97, Glu14, Ala70, Pro96 and Val73 forming two (2) hydrogen bond interactions with Ala70, Glu14; and veneparil forms one (1) hydrogen bonding with Gly143 and its amino acid interactions include Cys145, Gly143, Thr190, Glu189 and Phe140 while N3 standard have Leu50, Asp187, Thr25, Gln189, Glu166 as its amino acid interactions at the active site of the 6LU7 protein together with three (3) hydrogen bond interactions. Amino acid residues Glu166, Gln189; and Asp187 at the active site of 6LU7 formed three (3) hydrogen bonds with N3 standard. All drugs interacted with 2ZU4 and their interactions are listed above in Table 3. Lopinavir had interaction with 2ZU4 (2ZU4-Lopinavir Complex) at residues Glu110, Phe294, Pro293, Ile249, Leu202, and His246 forming one (1) hydrogen bond with Gln110; nelfinavir at Glu166, Glu189, Met49, His41, Cys145, Leu141, Asn142, Pro168, and Met165 with two (2) hydrogen bonds with Gln166 and Gln189; Indinavir at Cys145, Met49, His41, Glu166, His163, Phe140, Pro168, and Ala191 forming two (2) hydrogen bonds with Gln166 and His163; verapamil at His246, Ser158, Leu202, Ile249, Pro293, Thr292, and Phe294 forming two hydrogen bonds with His246 and Ser158; maraviroc at residues Leu167, Pro168, His163, and Cys145 with one (1) hydrogen bond with Gln166 and chlorophene at residues Gln110, Pro108, and Phe2. The standard 2-(acetylamino) 2-deoxy-A-D-glucopyranose interacted with 2ZU4 at Glu110, Pro108, and Phe294 while residues Try239 and Arg131 of 2ZU4 active site formed two (2) hydrogen bonds with the standard.

Table 4 shows the amino acid interactions of 6VSB protein and the drugs. Lopinavir interacted with 6VSB at amino acid residues Pro863, Lys733, His1058, Pro862, Ser730, and Val860; Maraviroc had its interaction at His401, Asp382, Ala348, His378, Lys562, Glu398, Phe390, Phe40, and Arg393 with one (1) hydrogen bond; nelfinavir had its interaction with 6VSB at His1058, Thr732, Pro863, Val860, and Ala956; indinavir at Thr549, Thr547, Thr572, Pro589, Phe592, Gly548, and Leu546 with two (2) hydrogen bonds, amodiaquine interacted with the protein at Gly283, Tyr38, Asp40, and Val42

forming three (3) hydrogen bonds while verapamil interacted with 6VSB at Thr1077, Ala713, Ile712, Tyr707, Ala1078, Pro1079, and Asn709 forming two (2) hydrogen bonds. Cys538 and Glu619 at the active pocket of 6VSB formed two hydrogen bonds with the standard. All the clinically approved drugs with the standard (2-(acetylamino) 2-deoxy-A-D-glucopyranose) interacted with 2AJF and the amino acids interactions are presented as Table 5 above. Indinavir interacted with 2AJF at residues Ser44, Arg514, Asp350, Asp382, and Trp349 with three (3) hydrogen bonds; saquinavir at His401, Asp382, Ala348, His378, Lys562, Glu398, Phe390, Phe40, and Arg393 with two (2) hydrogen bonds; lopinavir at Leu85, Asn103, Asn210, Lys94, Val212, Leu91, Leu95, Pro565, Glu98, and Trp196 with three (3) hydrogen bonds; maraviroc at Tyr385, His401, His378, Trp349, Trp69, Ser44, and Asp350 with three (3) hydrogen bonds; verapamil interacted with Trp349, Asn394, Phe40, Ala348, and Ser47 forming two (2) hydrogen bonds; and lastly chlorophene interacted with Trp349, His401, and Phe40 at the active site. The standard 2-(Acetylamino) 2-deoxy-A-D-glucopyranose interacted with 2AJF forming three (3) hydrogen bond interactions with Asp194, His195, and Asp103.

The molecular mechanism surrounding host cell and tissue interaction in virology involves receptor recognition. The mechanism of SARS-CoV-2 viral infection and replication involve its spike glycoproteins (S) which masterminds its entry into the cells and therefore serves as the main target for antibody<sup>24</sup>. Although, it was reported that SARS-CoV-2 spike glycoprotein exploits ACE2 for cell entry, it must be noted that the binding affinity of SARS-CoV for human ACE2 (hACE2) have significant correlation with the viral replication in some species in addition to transmissibility and disease severity<sup>25,26</sup>. It may also imply that SARS-CoV-2 infection and replication have critical relationship with human renin angiotensin system (RAS) which could lead to the provocation of cardiovascular complications. Therefore, small molecule that could interact/inhibit ACE2 might stand the chance of competing with SARS-CoV-2 at its ACE2 binding site. It was reported that SARS-CoV-2-mediated infection is been transmitted when SARS-CoV-2 virus exploits ACE2 as its binding receptor, it activates the RAS pathway that leads to the direct loss of ACE2, inoculating the respiratory mucosa cells thereby, acting as the functional receptor-channel for the viral entry. This consequently provokes viral pulmonary replication and indirect manifestation of COVID-19.<sup>27</sup>

The various interactions formed by indinavir, saquinavir, and lopinavir with 2AJF (SARS coronavirus spike binding domain otherwise called angiotensin converting enzyme 2) is an indication that these clinically approved antiviral drugs could be a potent inhibitor of human angiotensin converting enzyme 2 – the receptor for the spike glycoprotein of this deadly virus thereby blocking its attachment to the host cells and its subsequent downstream replication and signaling deleterious processes. Indinavir (-9.2 Kcal/mol), maraviroc (-9.1 Kcal/mol), and lopinavir (-8.5 Kcal/mol) had the highest binding energies against 2AJF. Amino acid residues Ser44, Asp350, and Trp349 are common to indinavir and maraviroc while His401, Ala348, His378, and Phe40 are common to saquinavir. It may imply that these amino acid residues contribute immensely to the catalytic potential of 2AJF or their synergistic potential might have contributed to their strong binding affinity expressed through their binding energies.

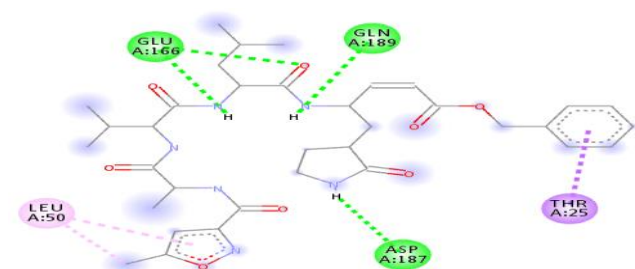
Lopinavir, maraviroc, and nelfinavir had the lowest binding energies with 6VSB, implying a probable strong binding affinity for the protein, therefore suggesting their propensity to inhibit the protein. Amino acid residues common to lopinavir and nelfinavir include Pro863, His1058, and Val860. So, it may be suggested that these amino acid residues might be critical to the catalytic functions of 6VSB and its attachment to its host for replication. It is noteworthy that all ligands expressed lower binding energies for 6VSB than their standard 2-(Acetylamino) 2-deoxy-A-D-glucopyranose, indicating that these ligands could be better inhibitors of 2AJF than the standard 2-(Acetylamino) 2-deoxy-A-D-glucopyranose.

It was reported that evolutionary similarities exist between SARS-CoV and SARS-CoV-2 through a Blast-mediated protein sequence alignment and this inference was evidenced by the 95%-100% homology.<sup>28</sup> Besides this, nucleocapsid protein N of SARS-CoV-2 expresses approximately 90% amino acid residue similarities with



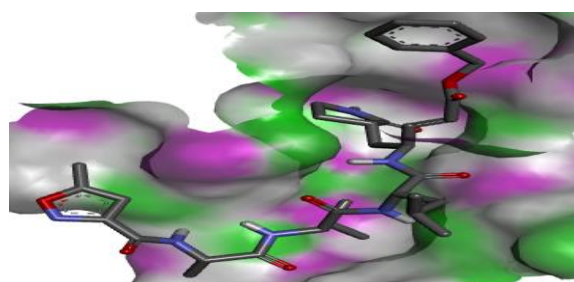
SARS-CoV<sup>29</sup> indicating that some drugs/ligands that could interact with or inhibit SARS-CoV-2 might also have affinity for SARS-CoV and vice versa. In addition, the S2 SARS-CoV-2 spike is reported to share 99% congruence with bat-SL-CoVZXC21, bat-SL-CoVZC45, and human SARS-CoV<sup>28</sup> meaning ligands that could inhibit one of these viral proteins could be a potential therapeutic inhibitor to the other. For 2ZU4 (SARS-CoV1 protease), all ligands exhibited stronger binding affinity than the standard Benzyl N-[(2S)-3-(2,2-dimethylpropanoylamino)-1-[[[(2S)-4-methyl-1-oxo-1-[(2R)-5-oxo-1-[(3S)-2-oxopyrrolidin-3-yl] hexan-2-yl]amino]pentan-2-yl]amino]-1-oxopropan-2-yl] carbamate. Lopinavir (2ZU4-Lopinavir complex) and verapamil (2ZU4-Verapamil complex) have Phe294, Pro293, Ile249, Leu202, and His246 residues as common interactions within their complexes while nelfinavir and indinavir have Glu166, Met49, His41, and Cys145 as their common residues. Just like others, these residues might contribute to the catalysis occurring within the complexes and they might have contributed to the binding affinities of the ligands to the protein. Lopinavir, nelfinavir, and indinavir showed the lowest binding energies with 2ZU4 and it must be noted that all ligands/drugs exhibited stronger binding affinities than the standard, meaning all

ligands are expected to be better inhibitors of SARS-CoV-1 viral replication. Maraviroc was the only drug with a slightly higher binding affinity with 6LU7 when compared with N3 standard, nelfinavir exhibited the same binding affinity. When the amino acids residues responsible for the interactions between 6LU7-N3 complex and 6LU7-maraviroc complex were compared, it was noticed that Asp187, Gln189, and Glu166 are all common to these two ligands/drugs while Gln189, His41, Cys145, and Met49 are the common amino acids of 6LU7-maraviroc and 6LU7-nelfinavir complexes. Furthermore, since 6LU7 and 2ZU4 codes for SARS-CoV-2 and SARS-CoV, we compared the amino acid residues common to their complexes (i.e 2ZU4-All ligands + Standard and 6LU7-All ligands + standard complexes) and we noticed that Glu166, Cys145, and Met49 are common to both complexes. Besides the fact that these amino acids could be critical to their structure and functional properties including their catalytic potentials, they might also be a part of their conserved residues. Our result falls in perspective with others where His41 and Cys145 were both reported to be conserved residues located at the Mpro (6LU7) active site catalytic dyad.<sup>30,31</sup>



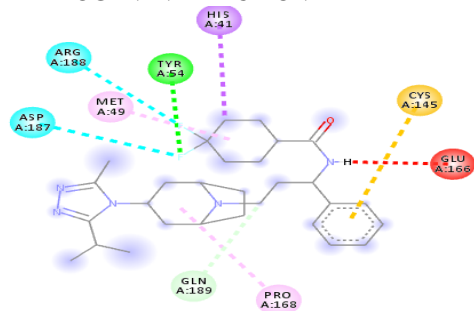
6LU7 HYDROGEN INTERACTION

N3 WITH



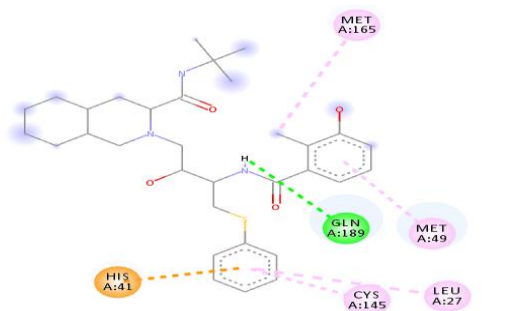
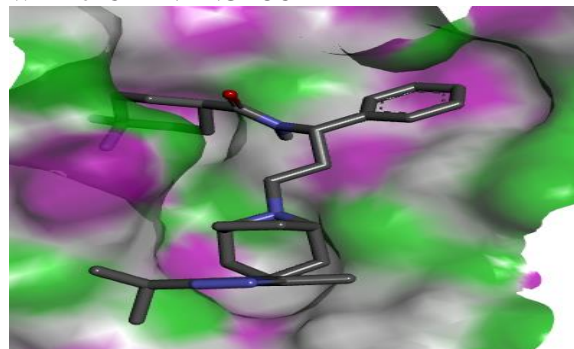
N3

WITH 6LU7 BINDING POCKET

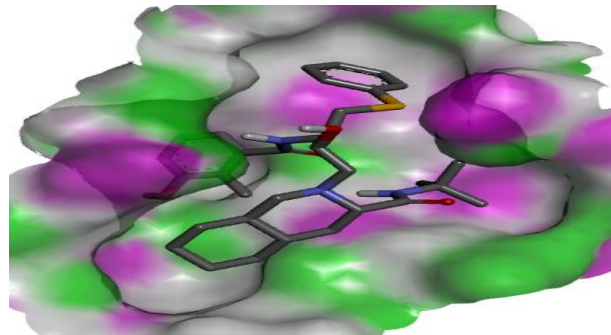


MARAVIROC WITH 6LU7 HYDROGEN INTERACTION

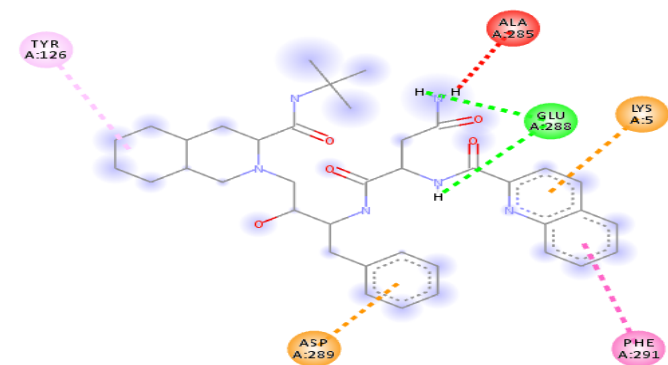
MARAVIROC WITH 6LU7 BINDING POCKET



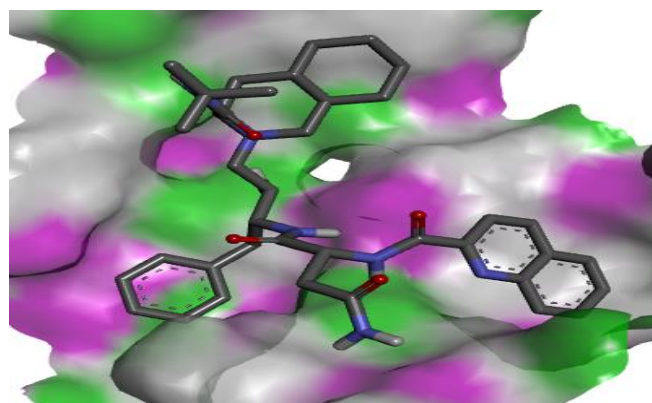
NELFINAVIR WITH 6LU7 HYDROGEN INTERACTION



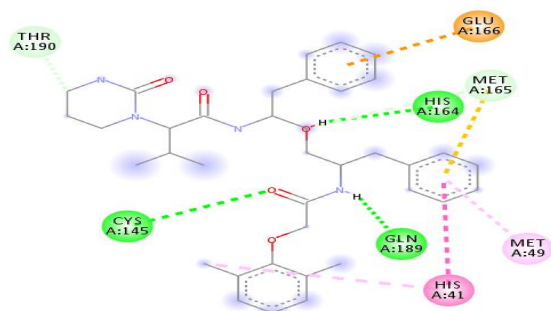
NELFINAVIR WITH 6LU7 BINDING POCKET



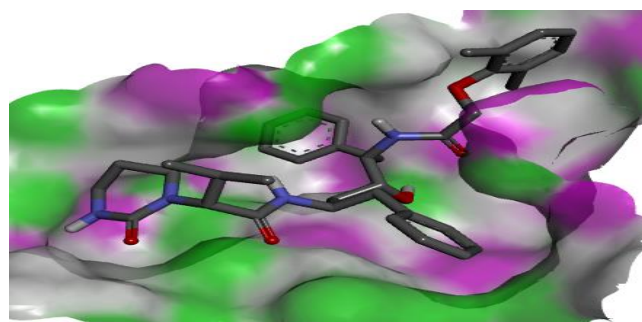
SAQUINIVIR WITH 6LU7 HYDROGEN INTERACTION



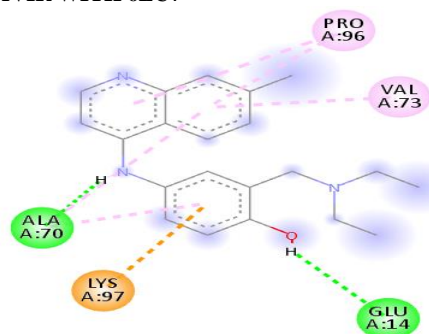
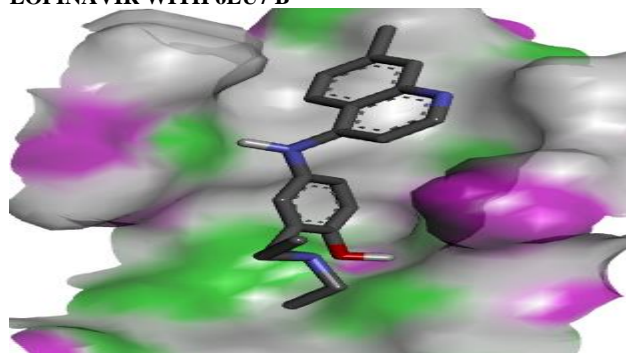
SAQUINIVIR WITH 6LU7 BINDING POCKET



LOPINAVIR WITH 6LU7

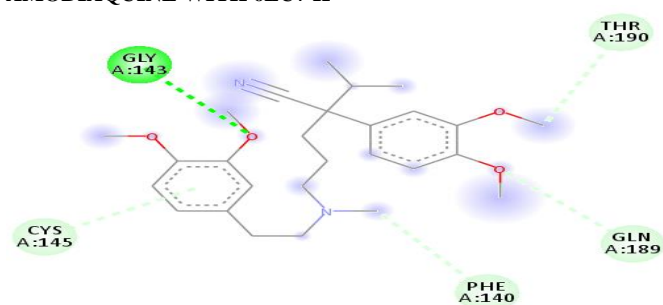
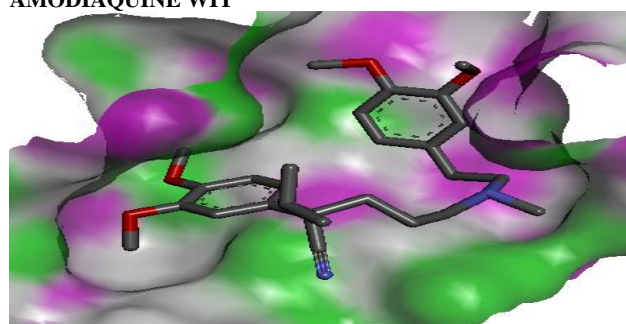


LOPINAVIR WITH 6LU7 B

HYDROGEN INTERACTION  
AMODIAQUINE WITH 6LU7 H

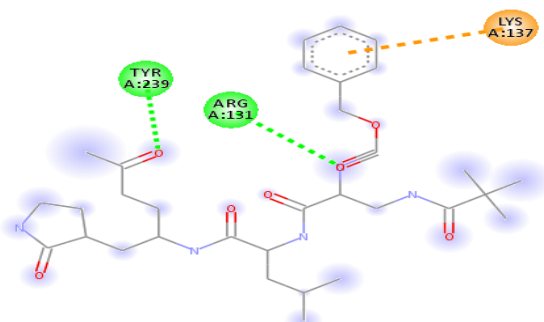
INDING POCKET

AMODIAQUINE WIT

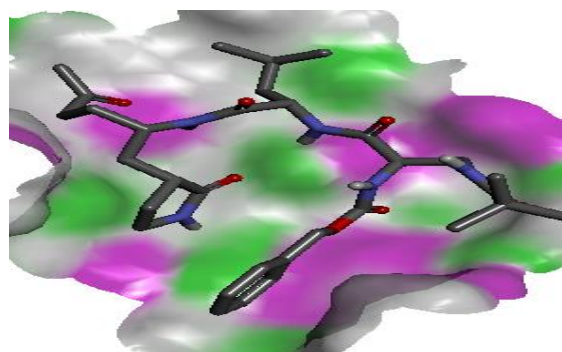
HYDROGEN INTERACTION VERAPAMIL WITH 6LU7 HYDROGEN  
INTERACTIONH 6LU7 BINDING POCKET VERAPAMIL WITH 6LU7  
BINDING POCKET

**Figure 2:** Representation of ligands docked with 6LU7 showing various interactions and their respective binding pockets.

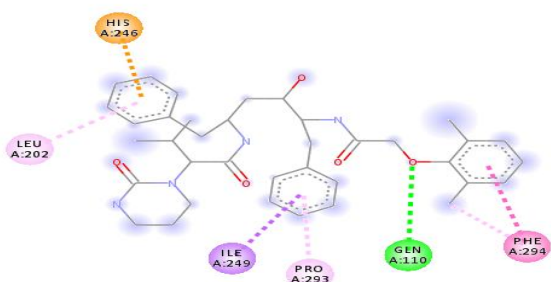




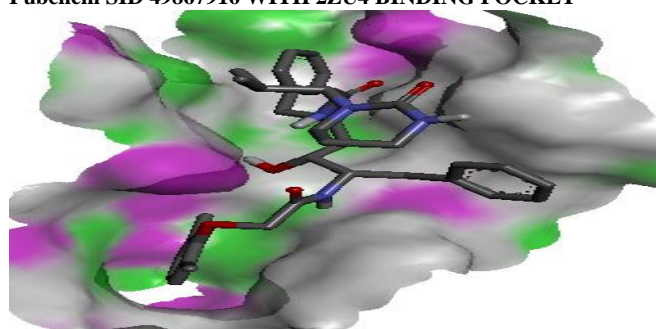
Pubchem SID 49867916 WITH 2ZU4 HYDROGEN INTERACTION



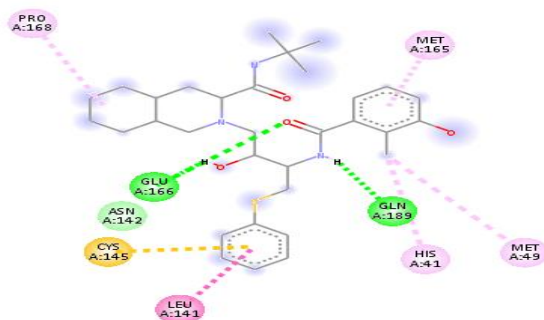
Pubchem SID 49867916 WITH 2ZU4 BINDING POCKET



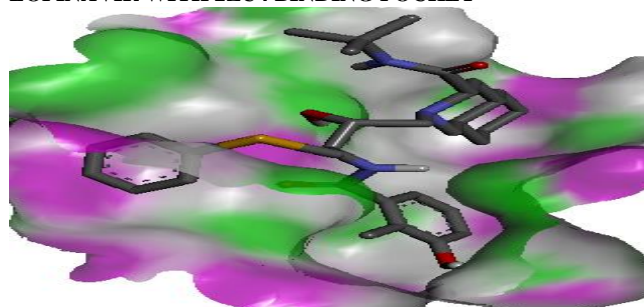
LOPINAVIR WITH 2ZU4 HYDROGEN INTERACTION



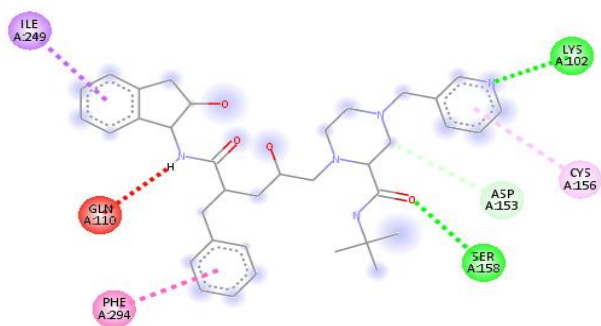
LOPINAVIR WITH 2ZU4 BINDING POCKET



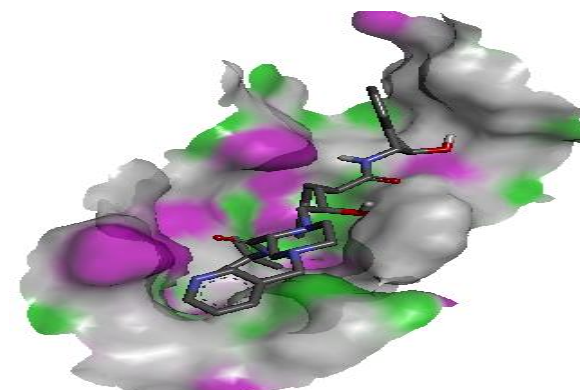
NELFINAVIR WITH 2ZU4 HYDROGEN INTERACTION



NELFINAVIR WITH 2ZU4 BINDING POCKET



INDINAVIR WITH 2ZU4 HYDROGEN INTERACTION



INDINAVIR WITH 2ZU4 BINDING POCKET

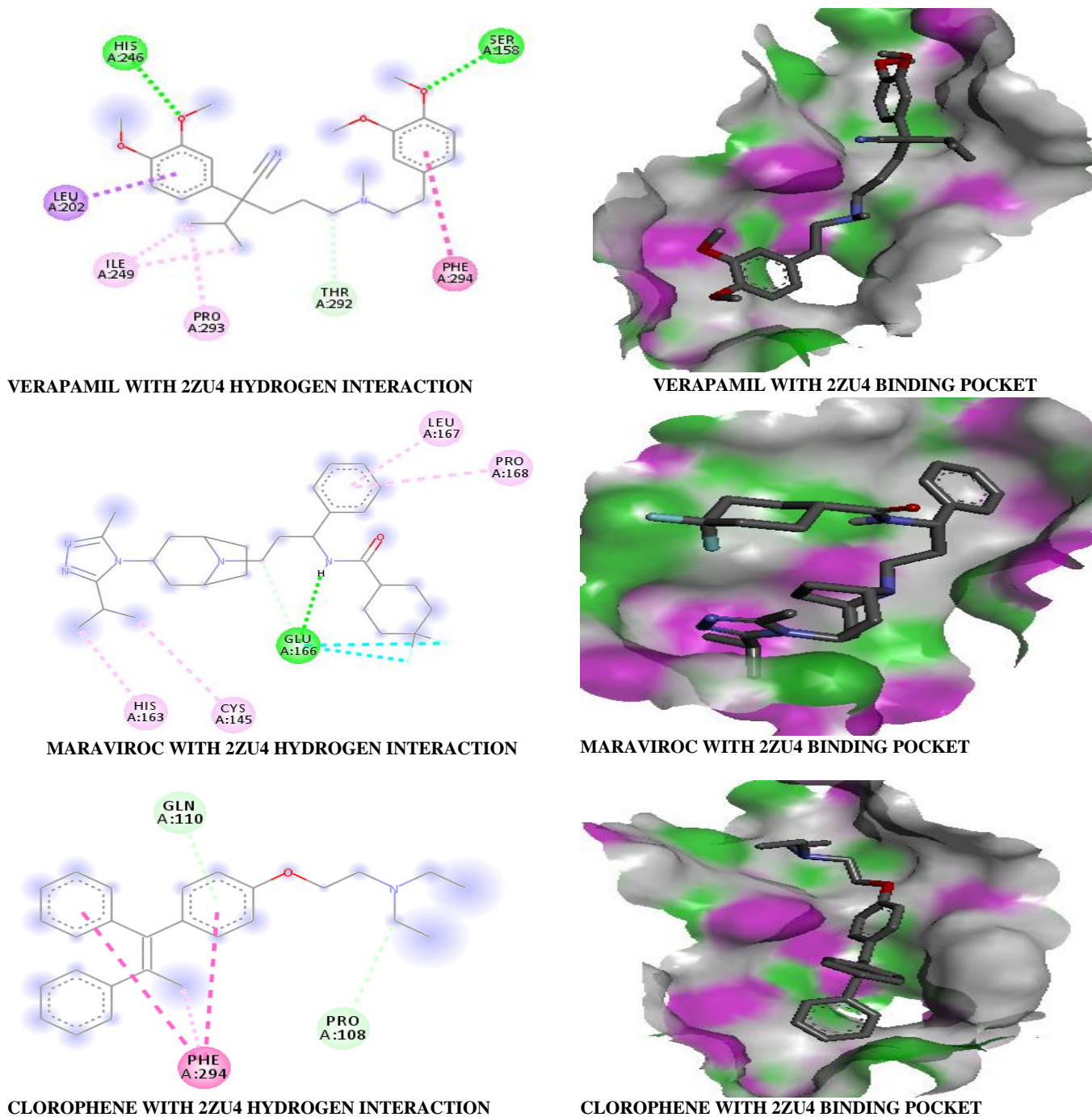
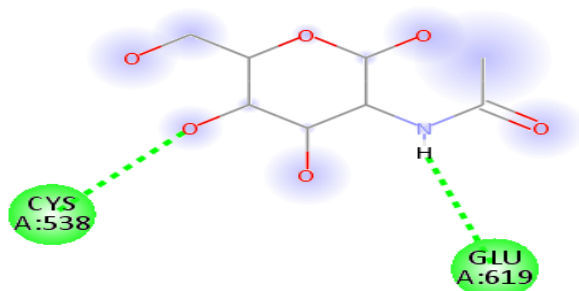
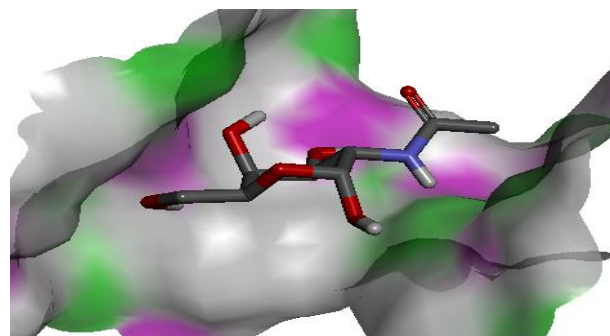


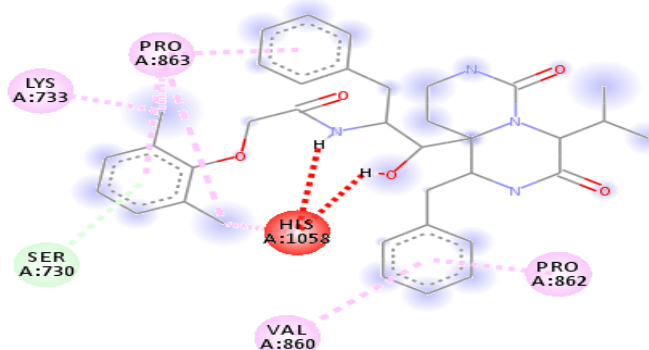
**Figure 3:** Representation of ligands binding to 2ZU4 showing various interactions and their respective binding pockets.



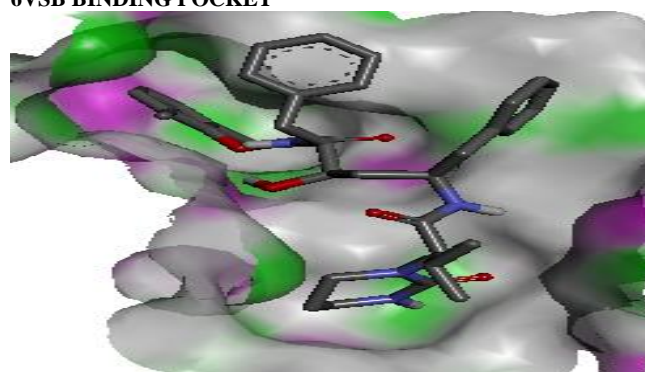
2-(ACETYLAMINO) 2-DEOXY-A-D-GLUCOPYRANOSE WITH 6VSB HYDROGEN INTERACTION



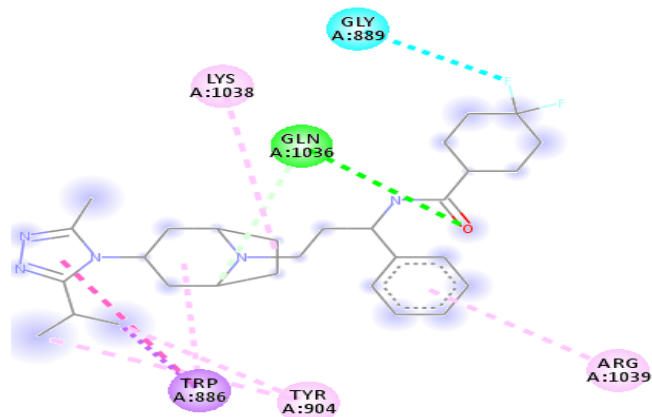
2-(ACETYLAMINO) 2-DEOXY-A-D-GLUCOPYRANOSE WITH 6VSB BINDING POCKET



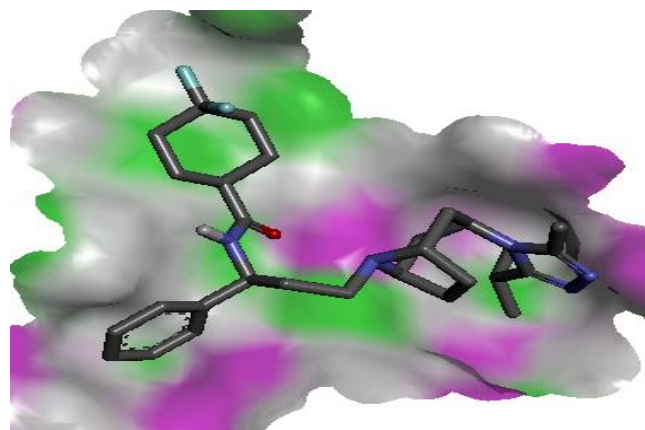
LOPINAVIR WITH 6VSB HYDROGEN INTERACTION



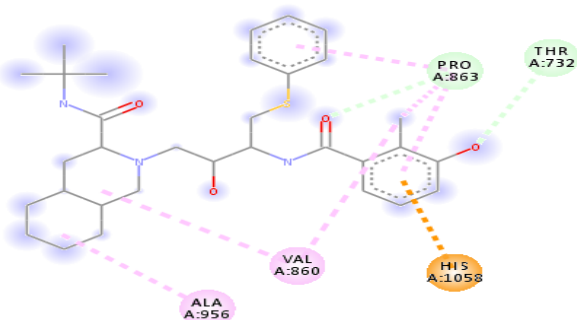
LOPINAVIR WITH 6VSB BINDING POCKET



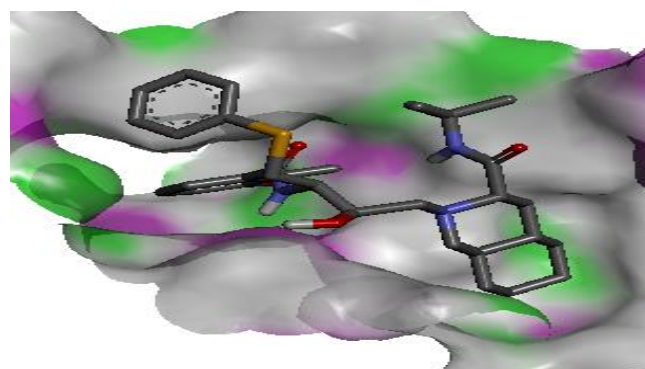
MARAVIROC WITH 6VSB HYDROGEN INTERACTION



MARAVIROC WITH 6VSB BINDING POCKET

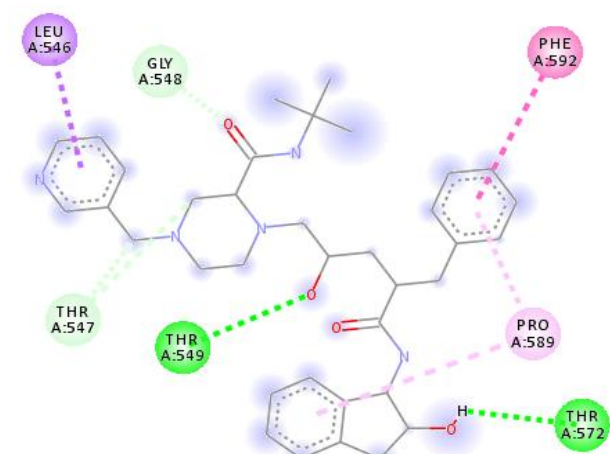


NELFINAVIR WITH 6VSB HYDROGEN INTERACTION

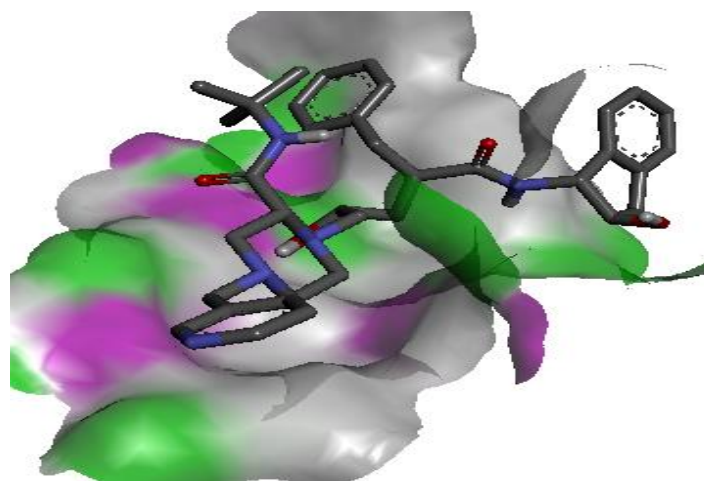


NELFINAVIR WITH 6VSB BINDING POCKET

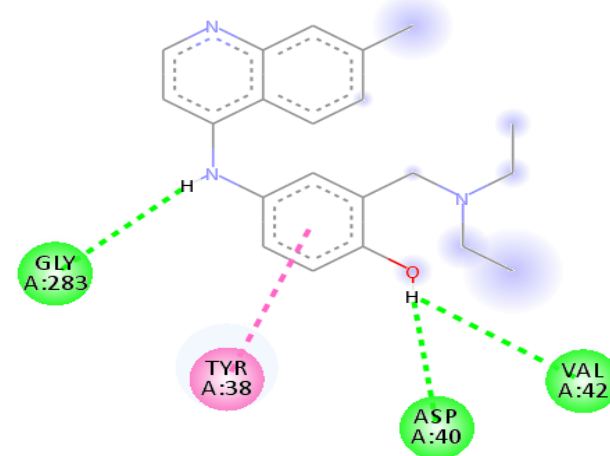




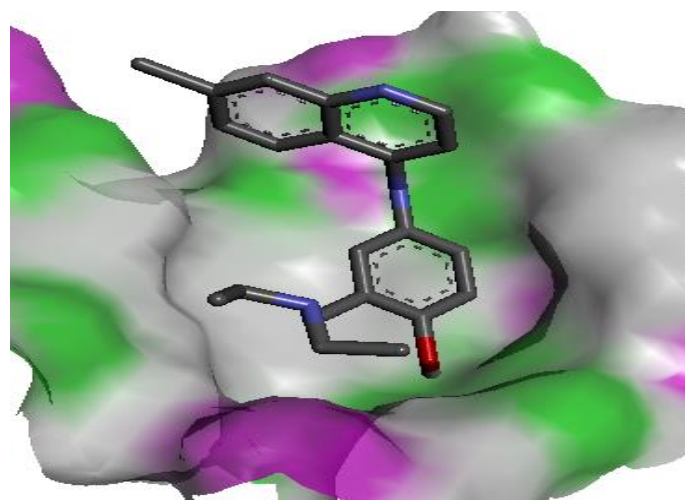
INDINAVIR WITH 6VSB HYDROGEN INTERACTION



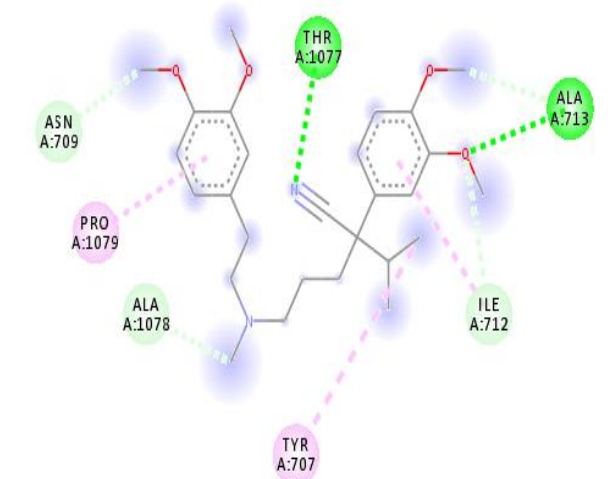
INDINAVIR WITH 6VSB BINDING POCKET



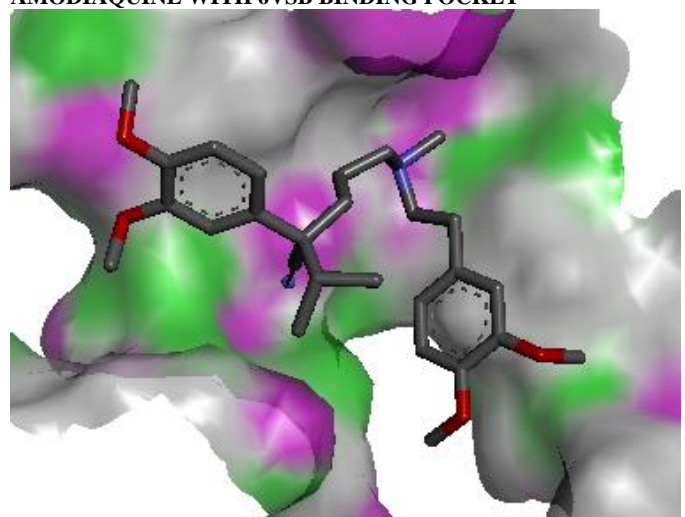
AMODIAQUINE WITH 6VSB HYDROGEN INTERACTION



AMODIAQUINE WITH 6VSB BINDING POCKET

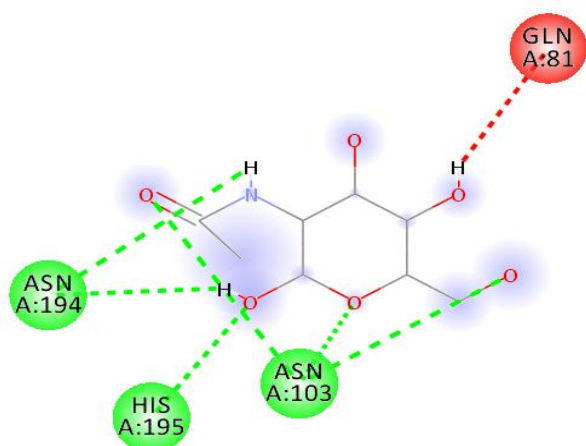


VERAPAMIL WITH 6VSB HYDROGENINTERACTION

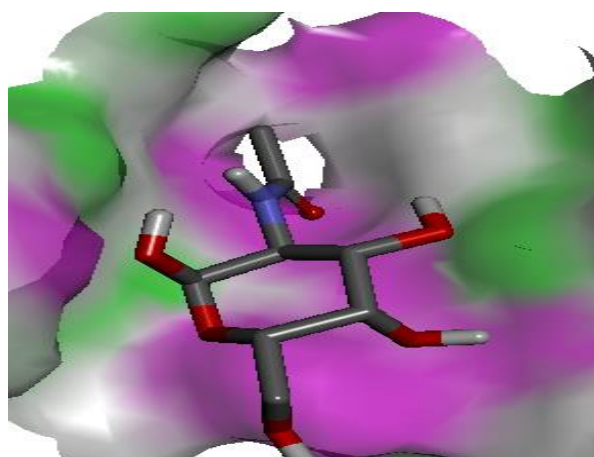


VERAPAMIL WITH 6VSB BINDING POCKET

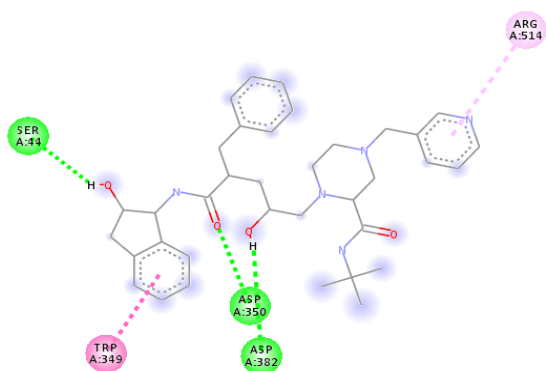
**Figure 4:** Representation of ligands with 6SVB and the various interactions hydrogen interactions and their respective binding pockets.



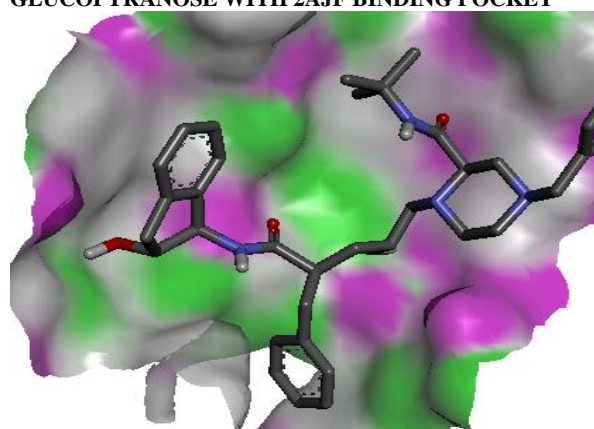
2-(ACETYLAMINO) 2-DEOXY-A-D-GLUCOPYRANOSE WITH 2AJF HYDROGEN INTERACTION



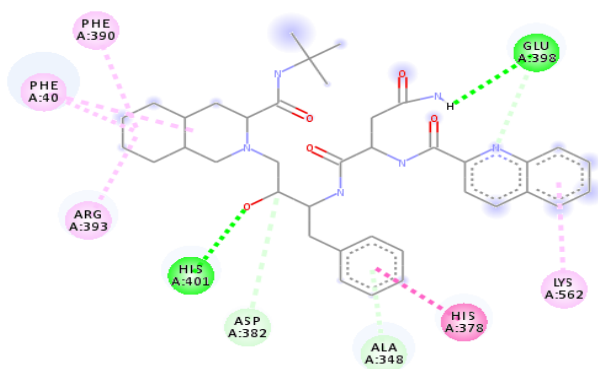
2-(ACETYLAMINO) 2-DEOXY-A-D-GLUCOPYRANOSE WITH 2AJF BINDING POCKET



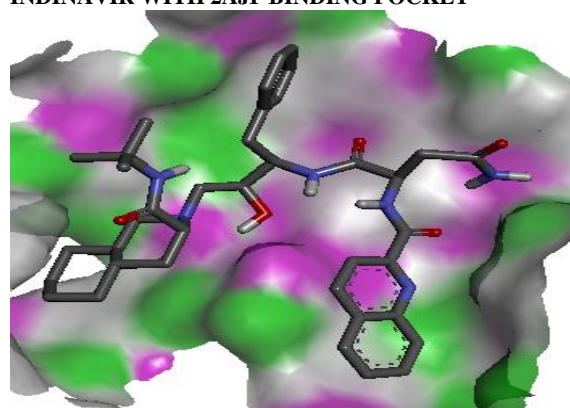
INDINAVIR WITH 2AJF HYDROGEN INTERACTION



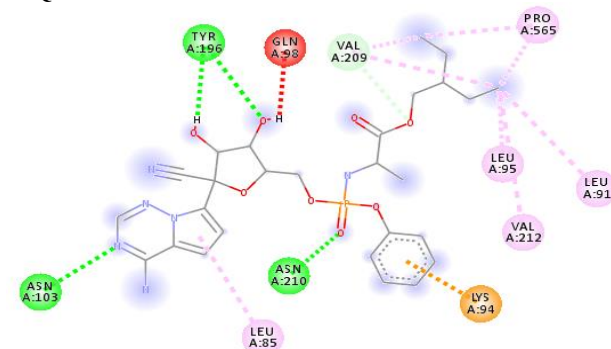
INDINAVIR WITH 2AJF BINDING POCKET



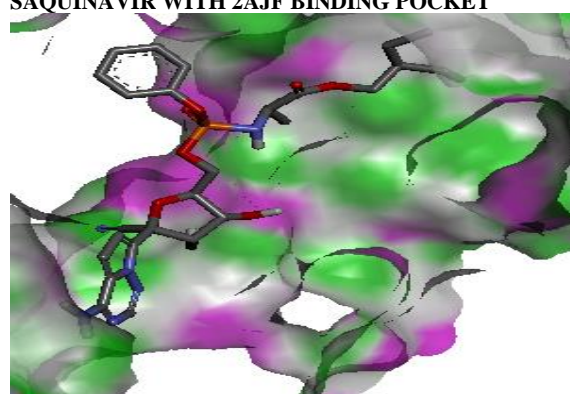
SAQUINAVIR WITH 2AJF HYDROGEN INTERACTION



SAQUINAVIR WITH 2AJF BINDING POCKET

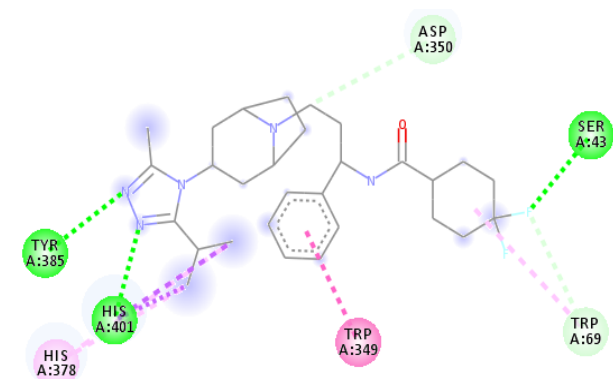


LOPINAVIR WITH 2AJF HYDROGEN INTERACTION

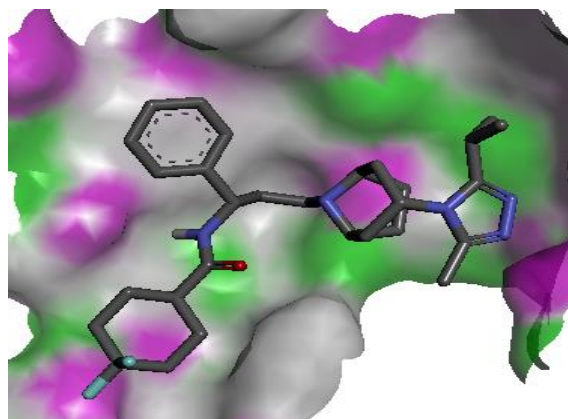


LOPINAVIR WITH 2AJF BINDING POCKET

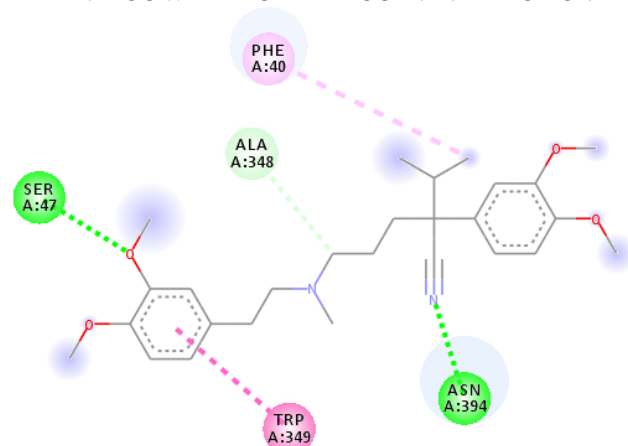




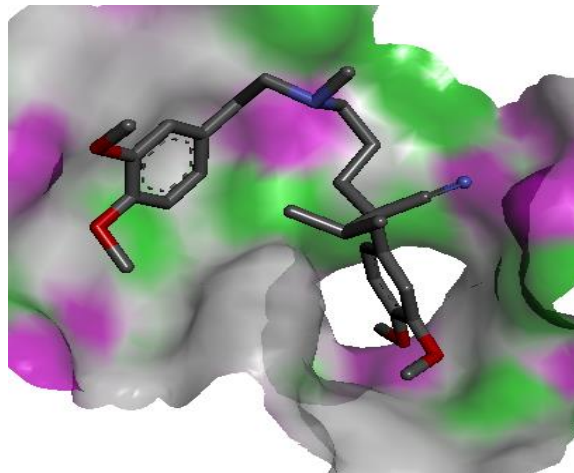
MARAVIROC WITH 2AJF HYDROGEN INTERACTION



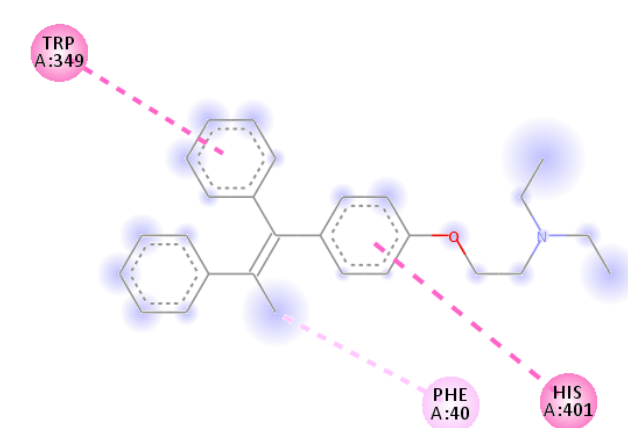
MARAVIROC WITH 2AJF BINDING POCKET



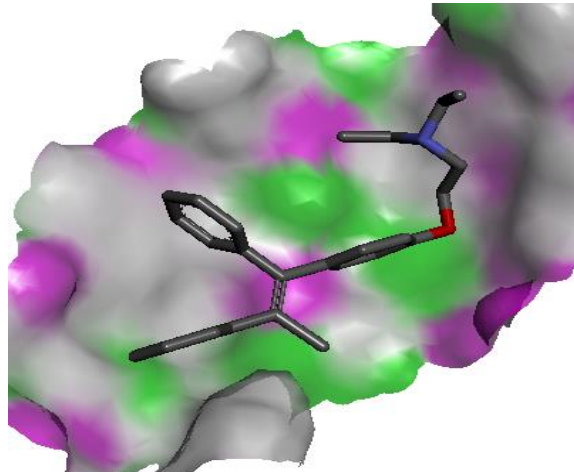
VERAPAMIL WITH 2AJF HYDROGEN INTERACTION



VERAPAMIL WITH 2AJF BINDING POCKET









CLOROPHENE WITH 2AJF HYDROGEN INTERACTION



CLOROPHENE WITH 2AJF BINDING POCKET

**Figure 5:** Representation of ligands with 2AJF and the expression of various interactions with their respective binding pockets**INTERACTIONS**

	CONVENTIONAL HYDROGEN BOND
	CARBON HYDROGEN BOND
	UNFAVOURABLE ACCEPTOR - ACCEPTOR

	Pi - Sulfur
	Pi-Pi Stacked
	Pi-Alkyl



**Table 1:** Binding Energies of clinically approved anti-retroviral, anti-ebola and anti-SARS drugs against 6LU7, 2ZU4, 6VSB and ACE2 Proteins

	ANTI-RETROVIRAL	ANTI-EBOLA	ANTI-SARS
<b>6LU7</b>	MARAVIROC (-7.7 Kcal/mol)	AMODIAQUINE (-6.0 Kcal/mol)	SAQUINAVIR (-7.5 Kcal/mol)
	LOPINAVIR (-7.1 Kcal/mol)	VERAPAMIL (-5.5 Kcal/mol)	NELFINAVIR (-6.3 Kcal/mol)
<b>2ZU4</b>	LOPINAVIR (-7.8 Kcal/mol)	VERAPAMIL (-7.4 Kcal/mol)	NELFINAVIR (-7.8 Kcal/mol)
	MARAVIROC (-7.2 Kcal/mol)	CLOROPHENE (-6.5 Kcal/mol)	SAQUINAVIR (-7.3 Kcal/mol)
<b>6VSB</b>	LOPINAVIR (-7.7 Kcal/mol)	AMODIAQUINE (-5.9 Kcal/mol)	NELFINAVIR (-7.1 Kcal/mol)
	MARAVIROC (-7.4 Kcal/mol)	VERAPAMIL (-5.4 Kcal/mol)	INDINAVIR (-6.8 Kcal/mol)
<b>2AJF</b>	MARAVIROC (-8.5 Kcal/mol)	VERAPAMIL (-6.8 Kcal/mol)	INDINAVIR (-9.2 Kcal/mol)
	LOPINAVIR (-8.3 Kcal/mol)	CLOROPHENE (-6.4 Kcal/mol)	SAQUINAVIR (-9.1 Kcal/mol)

**Table 2:** Number of hydrogen bond and amino acid interactions for 6LU7-ligand complexes

LIGANDS WITH 6LU7	NO OF HYDROGEN BOND	AMINO ACID INTERACTION WITH THEIR BOND LENGTH	BINDING ENERGY
N3	3	Leu50, Asp187, Thr25, Gln189, Glu166	-7.6 Kcal/mol
Maraviroc	1	Glu166, His41, Cys145, Met49, Pro168, Gln189, Tyr54, Arg188 Asp187	-7.7 Kcal/mol
Nelfinavir	1	Gln189, His41, Cys145, Leu27, Met49, Met165	-7.6 Kcal/mol
Saquinavir	1	Tyr126, Asp289, Phe291, Lys5, Ala285	-7.5 Kcal/mol
Lopinavir	3	Glu166, His41, Cys145, His164, Glu189, Met49, Thr190	-7.1 Kcal/mol
Amodiaquine	2	Lys97, Glu14, Ala70, Pro96, Val73	-6.0 Kcal/mol
Verapamil	1	Cys145, Gly143, Thr190, Glu189, Phe140	-5.5 Kcal/mol

**Table 3:** Number of hydrogen bond and amino acid interactions for 2ZU4-ligand complexes

Ligands with 2ZU4	NO OF H. BOND	AMINO ACID INTERACTION WITH THEIR BOND LENGTH	BINDING ENERGY
Benzyl N-[(2S)-3-(2,2-dimethylpropanoylamino)-1-[[[(2S)-4-methyl-1-oxo-1-[[[(2R)-5-oxo-1-[(3S)-2-oxopyrrolidin-3-yl]hexan-2-yl]amino]pentan-2-yl]amino]-1-oxopropan-2-yl]carbamate	2	Tyr239, Arg131, Lys137	-6.0 Kcal/mol
Lopinavir	1	Glu110, Phe294, Pro293, Ile249, Leu202, His246	-7.8 Kcal/mol
Nelfinavir	2	Glu166, Glu189, Met49, His41, Cys145, Leu141, Asn142, Pro168, Met165	-7.8 Kcal/mol
Indinavir	2	Cys145, Met49, His41, Glu166, His163, Phe140, Pro168, Ala191	-7.7 Kcal/mol
Verapamil	2	His246, Ser158, Leu202, Ile249, Pro293, Thr292, Phe294.	-7.4 Kcal/mol
Maraviroc	1	Leu167, Pro168, His163, Cys145	-7.2 Kcal/mol
Clorophene	0	Gln110, Pro108, Phe294	-6.5 Kcal/mol

**Table 4:** Number of hydrogen bond and amino acid interactions for 6VSB-ligand complexes

Ligands with 6VSB glycoprotein	No of H. Bond	Amino Acid Interaction with their Bond Length	Binding Energy
2-(Acetylamino) 2-deoxy-A-D-glucopyranose	2	Cys538, Glu619	-4.5 Kcal/mol
Lopinavir	0	Pro863, Lys733, His1058, Pro862, Ser730, Val860.	-7.7 Kcal/mol
Maraviroc	1	Gly889, Gln1036, Lys1038, Arg1039, Tyr904, Trp886	-7.4 Kcal/mol
Nelfinavir	0	His1058, Thr732, Pro863, Val860, Ala956	-7.1 Kcal/mol
Indinavir	2	Thr549, Thr547, Thr572, Pro589, Phe592, Gly548, Leu546.	-6.8 Kcal/mol
Amodiaquine	3	Gly283, Tyr38, Asp40, Val42	-5.9 Kcal/mol
Verapamil	2	Thr1077, Ala713, Ile712, Tyr707, Ala1078, Pro1079, Asn709.	-5.4 Kcal/mol

**Table 5:** Number of hydrogen bond and amino acid interactions for 2AJF-ligand complexes

Ligands with 2AJF	No of H. Bond	Amino Acid Interaction with their Bond Length	Binding Energy
2-(Acetylamino) 2-deoxy-A-D-glucopyranose	5	His195, Asn194, Asn103, Gln81	-5.3 Kcal/mol
Indinavir	3	Ser44, Arg514, Asp350, Asp382, Trp349	-9.2 Kcal/mol
Saquinavir	2	His401, Asp382, Ala348, His378, Lys562, Glu398, Phe390, Phe40, Arg393	-9.1 Kcal/mol
Maraviroc	3	Tyr385, His401, His378, Trp349, Trp69, Ser44, Asp350	-8.5 Kcal/mol
Lopinavir	3	Leu85, Asn103, Asn210, Lys94, Val212, Leu91, Leu95, Pro565, Glu98, Trp196	-8.3 Kcal/mol
Verapamil	2	Trp349, Asn394, Phe40, Ala348, Ser47	-6.8 Kcal/mol
Clorophene	0	Trp349, His401, Phe40	-6.4 Kcal/mol

## Conclusion

Amodiaquine, clomiphene, indinavir, lopinavir, maraviroc, nelfinavir, saquinavir, and verapamil were the best clinically approved antiviral drugs due to their binding energies against 6LU7, 2ZU4, 6VSB, and 2AJF. Therefore, as these clinically approved antiviral drugs might be good for the management/treatment of SARS-CoV-2-mediated COVID-19, we suggest Saquinavir, maraviroc, and nelfinavir might be the best set of drugs with good therapeutic efficacy than their respective standards. The reason surrounding this is because the binding energies they expressed against these proteins which was due to the different covalent interactions they formed with the amino acids at the active sites of these proteins signifies probable inhibitory propensities. However, further experimental assays are required to validate their potentials. They exhibited strong binding affinities but inhibitory activities can be confirmed by more computational analysis – Molinspiration for prediction of bioactivity and molecular dynamic simulation.

## Conflict of interest

The authors declare no conflict of interest.

## Authors' Declaration

The authors hereby declare that the work presented in this article is original and that any liability for claims relating to the content of this article will be borne by them.

## References

- Shereen MA, Khan S, Kazmi A, Bashir N, Siddique R. COVID-19 infection: Origin, transmission, and characteristics of human coronaviruses. *J Adv Res.* 2020; 16(24):91-98.
- Chan JF, Yuan S, Kok KH, To KK, Chu H, Yang J, Xing F, Liu J, Yip CC, Poon RW, Tsoi HW, Lo SK, Chan KH, Poon VK, Chan WM, Ip JD, Cai JP, Cheng VC, Chen H, Hui CK, Yuen KY. A familial cluster of pneumonia associated with the 2019 novel coronavirus indicating person-to-person transmission: a study of a family cluster. *Lancet.* 2020; 15(395):514-523.
- Mackenzie JS and Smith DW. COVID-19: a novel zoonotic disease caused by a coronavirus from China: what we know and what we don't. *Microbiol Aust.* 2020; 17:MA20013.
- Han Y, Du J, Su H, Zhang J, Zhu G, Zhang S, Wu Z and Jin Q. Identification of Diverse Bat Alphacoronaviruses and Betacoronaviruses in China Provides New Insights into the Evolution and Origin of Coronaviruses-Related Diseases. *Front Microbiol.* 2019; 10(15):19-25.
- Lu H, Stratton CW, Tang YW. Outbreak of pneumonia of unknown etiology in Wuhan China: the mystery and the miracle. *J Med Virol.* 2020; 92(4):401-402.
- Wang D, Hu B, Hu C, Zhu F, Liu X, Zhang J, Wang B, Xiang H, Cheng Z, Xiong Y, Zhao Y, Li Y, Wang X, Peng Z. Clinical Characteristics of 138 Hospitalized Patients With 2019 Novel Coronavirus-Infected Pneumonia in Wuhan, China. *JAMA.* 2020; 323(11):1061-1069.
- Li Q, Guan X, Wu P, Wang X, Zhou L, Tong Y, Ren R, Leung KSM, Lau EHY, Wong JY, Xing X, Xiang N, Wu Y, Li C, Chen Q, Li D, Liu T, Zhao J, Liu M, Tu W, Chen C, Jin L, Yang R,

- Wang Q, Zhou S, Wang E, Liu H, Luo Y, Liu Y, Shao G, Li H, Tao Z, Yang Y, Deng Z, Liu B, Ma Z, Zhang Y, Shi G, Lam TTY, Wu JT, Gao GF, Cowling BJ, Yang B, Leung GM, Feng Z. Early transmission dynamics in Wuhan, China, of novel coronavirus-infected pneumonia. *N Engl J Med*. 2020; 382(13):199-207.
8. Coronaviridae Study Group of the International Committee on Taxonomy of Viruses. The species Severe acute respiratory syndrome-related coronavirus: classifying 2019-nCoV and naming it SARS-CoV-2. *Nat Microbiol*. 2020; 5(4):536-544.
  9. Chen N, Zhou M, Dong X, Qu J, Gong F, Han Y, Qiu Y, Wang J, Liu Y, Wei Y, Xia J, Yu T, Zhang X, Zhang L. Epidemiological and clinical characteristics of 99 cases of 2019 novel coronavirus pneumonia in Wuhan, China: a descriptive study. *Lancet*. 2020; 395(10223):507-513.
  10. Huang C, Wang Y, Li X, Ren L, Zhao J, Hu Y, Zhang L, Fan G, Xu J, Gu X, Cheng Z, Yu T, Xia J, Wei Y, Wu W, Xie X, Yin W, Li H, Liu M, Xiao Y, Gao H, Guo L, Xie J, Wang G, Jiang R, Gao Z, Jin Q, Wang J, Cao B. Clinical features of patients infected with 2019 novel coronavirus in Wuhan, China. *Lancet*. 2020; 395(10223):497-506.
  11. Ge XY, Li JL, Yang XL, Chmura AA, Zhu G, Epstein JH, Mazet JK, Hu B, Zhang W, Peng C, Zhang YJ, Luo CM, Tan B, Wang N, Zhu Y, Cramer G, Zhang SY, Wang LF, Daszak P, Shi ZL. Isolation and characterization of a bat SARS-like coronavirus that uses the ACE2 receptor. *Nature*. 2013; 503(7477):535-8.
  12. Lu R, Zhao X, Li J, Niu P, Yang B, Wu H, Wang W, Song H, Huang B, Zhu N, Bi Y, Ma X, Zhan F, Wang L, Hu T, Zhou H, Hu Z, Zhou W, Zhao L, Chen J, Meng Y, Wang J, Lin Y, Yuan J, Xie Z, Ma J, Liu WJ, Wang D, Xu W, Holmes EC, Gao GF, Wu G, Chen W, Shi W, Tan W. Genomic characterisation and epidemiology of 2019 novel coronavirus: implications for virus origins and receptor binding. *Lancet*. 2020; 395(10224):565-574.
  13. Wu F, Zhao S, Yu B, Chen YM, Wang W, Song ZG, Hu Y, Tao ZW, Tian JH, Pei YY, Yuan ML, Zhang YL, Dai FH, Liu Y, Wang QM, Zheng JJ, Xu L, Holmes EC, Zhang YZ. A new coronavirus associated with human respiratory disease in China. *Nature*. 2020; 579(7798):265-269.
  14. Yelin Han, Jiang Du, Haoxiang Su, Junpeng Zhang, Guangjian Zhu, Shuyi Zhang, Zhiqiang Wu, and Qi Jin. Characterization of a filovirus (Mengla virus) from Rousettus bats in China. *Nat Microbiol*. 2019; 4:390-395.
  15. Sheahan TP, Sims AC, Leist SR, Schäfer A, Won J, Brown AJ, Montgomery SA, Hogg A, Babusis D, Clarke MO, Spahn JE, Bauer L, Sellers S, Porter D, Feng JY, Cihlar T, Jordan R, Denison MR, Baric RS. Comparative therapeutic efficacy of remdesivir and combination lopinavir, ritonavir, and interferon beta against MERS-CoV. *Nat Commun*. 2020; 11(1):222.
  16. Holshue ML, DeBolt C, Lindquist S, Lofy KH, Wiesman J, Bruce H, Spittes C, Ericson K, Wilkerson S, Tural A, Diaz G, Cohn A, Fox L, Petal A, Gerber SI, Kim L, Tong S, Lu X, Lindstrom S, Pallansch MA, Welson WC, Biggs-Hm, Uyeki TM, Pillai SK. Washington State 2019-nCoV Case Investigation Team. First case of 2019 novel coronavirus in the United States. *N Engl J Med*. 2020; 384(10):929-936.
  17. Wang M, Cao R, Zhang L, Yang X, Liu J, Xu M, Shi Z, Hu Z, Zhong W, Xiao G. Remdesivir and chloroquine effectively inhibit the recently emerged novel coronavirus (2019-nCoV) in vitro. *Cell Res*. 2020; 30(3):269-271.
  18. Cao YC, Deng QX, Dai SX. Remdesivir for severe acute respiratory syndrome coronavirus 2 causing COVID-19: An evaluation of the evidence. *Travel Med Infect Dis*. 2020; 35:101647.
  19. Chan JF, Kok KH, Zhu Z, Chu H, To KK, Yuan S, Yuen KY. Genomic characterization of the 2019 novel human-pathogenic coronavirus isolated from a patient with atypical pneumonia after visiting Wuhan. *Emerg Microbes Infect*. 2020; 9(1):221-236.
  20. Yuan Y, Cao D, Zhang Y, Ma J, Qi J, Wang Q, Lu G, Wu Y, Yan J, Shi Y, Zhang X, Gao GF. Cryo-EM structures of MERS-CoV and SARS-CoV spike glycoproteins reveal the dynamic receptor binding domains. *Nat Commun*. 2017; 8:15092.
  21. Walls AC, Xiong X, Park YJ, Tortorici MA, Snijder J, Quispe J, Cameroni E, Gopal R, Dai M, Lanzavecchia A, Zamboni M, Rey FA, Corti D, Veerles D. Unexpected Receptor Functional Mimicry Elucidates Activation of Coronavirus Fusion. *Cell*. 2019; 176(5):1026-1039.
  22. Trott O and Olson AJ. AutoDock Vina: improving the speed and accuracy of docking with a new scoring function, efficient optimization, and multithreading. *J Comput Chem*. 2010; 31(2):455-461.
  23. Computed Atlas for Surface Topography of Proteins (CASTp) (<http://sts.bioe.uic.edu/castp/index.html?2011>)
  24. Walls AC, Park YJ, Tortorici MA, Wall A, McGuire AT, Veerles D. Structure, Function, and Antigenicity of the SARS-CoV-2 Spike Glycoprotein. *Cell*. 2020; 181(2):281-292.
  25. Li W, Zhang C, Sui J, Kuhn JH, Moore MJ, Luo S, Wong SK, Huang IC, Xu K, Vasilieva N, Murakami A, He Y, Marasco WA, Guan Y, Choe H, Farzan M. Receptor and viral determinants of SARS-coronavirus adaptation to human ACE2. *EMBO J*. 2005; 24(8):1634-1643.
  26. Wan Y, Shang J, Graham R, Baric RS, Li F. Receptor Recognition by the Novel Coronavirus from Wuhan: an Analysis Based on Decade-Long Structural Studies of SARS Coronavirus. *J Virol*. 2020; 94(7):e00127-20.
  27. Gheblawi M, Wang K, Viveiros A, Nguyen Q, Zhong JC, Turner AJ, Raizada MK, Grant MB, Oudit GY. Angiotensin-Converting Enzyme 2: SARS-CoV-2 Receptor and Regulator of the Renin-Angiotensin System: Celebrating the 20th Anniversary of the Discovery of ACE2. *Circ Res*. 2020; 126(10):1456-1474.
  28. Chan JF, Kok KH, Zhu Z, Chu H, To KK, Yuan S, Yuen KY. Genomic characterization of the 2019 novel human-pathogenic coronavirus isolated from a patient with atypical pneumonia after visiting Wuhan. *Emerg Microbes Infect*. 2020; 9(1):221-236.
  29. Gralinski LE, Menachery VD. Return of the Coronavirus: 2019-nCoV. *Viruses*. 2020; 12(2):135.
  30. Hilgenfeld R. From SARS to MERS: crystallographic studies on coronaviral proteases enable antiviral drug design. *FEBS J*. 2014; 281(18):4085-96.
  31. Palese LL. The Structural Landscape of SARS-CoV-2 Main Protease: Hints for Inhibitor Search. *ChemRxiv*. 2020; 4(10):44-49.
  32. against the cowpea beetle, *Callosobruchus maculatus* (Fabricius). *Biopest Int*. 2011; 7(1):15-23.
  33. Anioke I, Okwuosa C, Uchendu I, Chijioke O, Dozie-Nwakile O, Ikegwuonu I, Kalu P, Okafor M. Investigation into Hypoglycemic, Antihyperlipidemic, and Renoprotective Potentials of *Dennettia tripetala* (Pepper Fruit) Seed in a Rat Model of Diabetes. *BioMed Res Int*. 2017; 2017.